

THE GEOLOGY AND GEOTHERMAL SETTING
OF THE MAGIC RESERVOIR AREA,
BLAINE AND CAMAS COUNTIES, IDAHO

Debra W. Struhsacker
Paul W. Jewell
Jon Zeisloft
Stanley H. Evans, Jr.¹

Earth Science Laboratory
University of Utah Research Institute
420 Chipeta Way Suite 120
Salt Lake City, Utah 84108

¹Department of Geology and Geophysics
University of Utah
Salt Lake City, Utah 84108

June, 1981

TABLE OF CONTENTS

	<u>Page</u>
Abstract
Introduction
Stratigraphy
Older Rhyolite of Magic Reservoir
Square Mountain Basalt.
Rhyolite Ash-Flow Tuffs of Magic Reservoir.
Tuff 1
Tuff 2
Tuff 3
Pumice of Magic Reservoir.
Source Area for the Magic Reservoir Rhyolite Ash-Flow Tuffs
Rhyolite Dome
Quaternary Sediments, Sedimentary Rocks, and Basalts.
Myrtle Sediments
Quaternary Basalts
Macon Sediments.
Unnamed Quaternary Conglomerate.
Quaternary Alluvium.
Structure. :
Comparison of the Magic Reservoir Rhyolites to Other Nearby Silicic Volcanic Rocks
Regional Volcanic Stratigraphy and Age Relationships of the Magic Reservoir Rhyolites.
Regional Significance of the Magic Reservoir Rhyolites
Geothermal Geology of the Magic Reservoir Area
Summary and Suggestions for Additional Work.
Acknowledgements
References Cited

LIST OF FIGURES

- Figure 1. Index Map of the Magic Reservoir Area
- Figure 2. Diagrammatic Stratigraphic Column for the Magic Reservoir Area
- Figure 3. Geologic Map and Cross Sections of the Magic Reservoir Area
- Figure 4. Physiographic Map of the Magic Reservoir Region
- Figure 5. Space-Time Profile of Volcanic Rocks Along the Snake River Plain, Idaho (modified after Armstrong and others, 1980)
- Figure 6. Idealized Cross Section and Temperature-Depth Profiles of a Geothermal Convection System (isotherms modified after Wilson and Chapman, 1980)
- Figure 7. The Relationship of Theoretical Conductive Cooling Models to Age, Size and Shape of Selected Young Igneous Systems in Idaho and Wyoming (modified after Smith and Shaw, 1979)

LIST OF TABLES

- Table 1. Petrographic Descriptions of the Rhyolites and Basalts at Magic Reservoir
- Table 2. Chemical Composition of Magic Reservoir and Other Snake River Plain Rhyolites
- Table 3. K-Ar Dates and Analytical Data for the Magic Reservoir Rhyolites

ABSTRACT

The Magic Reservoir area straddles the Blaine-Camas county line in south-central Idaho, along the northern boundary of the central Snake River Plain. The rocks exposed at Magic Reservoir include a 5.98 ± 0.69 m.y. old rhyolite flow, the Pliocene Square Mountain basalt, multiple cooling units of 5.85 ± 0.23 m.y. old rhyolite ash-flow tuff, a 4.94 ± 0.29 m.y. old rhyolite dome, and Quaternary basalt flows and sediments. These newly reported ages for the rhyolites at Magic Reservoir reveal that they are the youngest, westernmost silicic volcanic rocks presently known in the Snake River Plain. They represent an anomalously young rhyolitic event that may include the Moonstone Mountain rhyolite dome to the northwest and the previously dated (Armstrong and others, 1975) 3.06 ± 0.04 m.y. old Wedge Butte rhyolite dome to the southeast of Magic Reservoir.

The area is cut by numerous normal faults trending northwest, northeast, and west. The northwest-trending faults are the dominant structures. They form a horst block at Hot Springs Landing and parallel the regional structural grain.

The geothermal resource at Magic Reservoir occurs within the elevated heat flow province at the northern margin of the Snake River Plain. The system is probably controlled by deep, convective circulation of fluids along faults at the intersection of the Hot Springs Landing horst with west- and northeast-trending fractures. Although the volcanic rocks in the Magic Reservoir area are young,

they are too old to contribute any magmatic heat to the geothermal system.

INTRODUCTION

A study of the geology of the Magic Reservoir area (Figure 1) was undertaken in order to evaluate the Magic Reservoir geothermal system. The rocks in the Magic Reservoir area are primarily Pliocene to Quaternary rhyolites and basalts which are cut by numerous normal faults. The Magic Reservoir geothermal system consists of a 79 m deep well that produces 57 l/min of 71°C (160°F) water (Mitchell and others, 1980).

In order to understand the relationship between the Magic Reservoir geothermal system and the volcanic history of the region, the study area was examined in detail by means of geologic mapping on 1:20,000 scale aerial photographs, petrographic interpretation, whole-rock chemical analysis and K-Ar age dating. This paper attempts to place the Magic Reservoir volcanic rocks in the regional volcanic stratigraphic framework of the Snake River Plain. The mineralogy and composition of the Magic Reservoir rhyolitic rocks are compared to other nearby silicic volcanic rocks. K-Ar dates for the Magic Reservoir rhyolites contribute new data to the volcanic chronology of the western Snake River Plain. An analysis of the Magic Reservoir geothermal system both identifies the structures controlling geothermal fluid circulation and places this system within the context of the regional heat flow regime of the western Snake River Plain.

Previous geologic work in the Magic Reservoir area includes Schmidt's (1961) study of the Quaternary stratigraphy, Malde and

others' (1963) reconnaissance-scale map of the west-central Snake River Plain, and Smith's (1966) investigation of the Idavada volcanics in the eastern Mount Bennett Hills. Ross (1971), Mitchell (1976), and Mitchell and others (1980) briefly discuss the geothermal system at Magic Reservoir.

STRATIGRAPHY

Lithologies at Magic Reservoir (Figure 2) consist mainly of basalts and rhyolites, the bimodal volcanic assemblage characteristic of the Snake River Plain. The oldest rock exposed in the area is a coarsely porphyritic rhyolite lava flow, locally overlain by flows of Square Mountain Basalt. The next youngest rock at Magic Reservoir is a multiple cooling unit rhyolite ash-flow tuff. These ash-flow tuffs are cut by the feeder zone of a rhyolite dome. Quaternary basalt flows and sediments are the youngest rocks in the area.

Older Rhyolite of Magic Reservoir

The older rhyolite of Magic Reservoir is locally exposed in the northern and southeastern portions of the map area (Figure 3). It commonly forms rounded, hummocky outcrops. On the north side it is immediately overlain by the base of the ash-flow tuffs, a relationship best exposed 0.25 km west-northwest of Hot Springs Landing (Figure 4) where a knob of the older rhyolite is overlain by the nonwelded, porous base of the ash-flow tuffs. On the southeastern side of the area, the older rhyolite is overlain by the Square Mountain Basalt except where irregular paleo-topographic highs of the older rhyolite locally protruded above the basalt flows and were buried by the ash-flow tuffs.

The older rhyolite is coarsely porphyritic, with phenocrysts measuring up to 15 mm in length. The phenocryst content ranges from 40 to 50 percent and is comprised mainly of sanidine, quartz, and

lesser amounts of plagioclase. The groundmass texture varies from glassy to completely devitrified. The glassy variety is generally restricted to the upper portions of the unit, and is locally vesicular. Field relationships suggest that the older rhyolite is probably a blocky lava flow. A petrographic description of the older rhyolite is included in Table 1. The chemical composition of this unit is shown in Table 2.

Square Mountain Basalt

A unit of porphyritic basalt occurs in the Clay Bank Hills (Figure 4), where a thickness of at least 100 m is exposed in a prominent fault scarp overlooking Magic Reservoir. Exposures of the basalt in the Clay Bank Hills become progressively thinner to the north and are totally absent in the vicinity of Hot Springs Landing. Additional outcrops of the basalt are mapped north of the Landing by both Schmidt (1961) and Malde and others (1963). Malde and others (1963) map this unit as a part of the Banbury Basalt. Schmidt (1961) names it the Square Mountain Basalt after the type location at Square Mountain, 10 km northwest of Hot Springs Landing (Figure 4). The name Square Mountain Basalt is adopted for the purposes of this report.

In the study area, the Square Mountain Basalt is massive with no clearly defined flows or columnar jointing. The rock is locally vesicular, although vesiculation does not define recognizable flow horizons. The basalt is dark-gray to bluish-black and contains distinctive subround feldspar phenocrysts, 5 to 10 mm long, which have cleavage faces with a dull luster. Smaller (1 mm long) plagioclase laths are observed locally. Quartz phenocrysts, 1 to 2 mm in diameter, are present in trace amounts and have a characteristic greenish-brown tint. See Table 1 for a petrographic description of this basalt.

The thickening of the Square Mountain Basalt from north to south in the Clay Bank Hills and its absence around Hot Springs Landing could be due to the presence of an erosional paleo-topographic high of

the older volcanics prior to eruption of the Square Mountain Basalt, or localized erosion of the basalt prior to eruption of the overlying ash-flow tuffs. An alternative explanation is that the basalt north of Hot Springs Landing erupted from Square Mountain while the basalt in the Clay Bank Hills erupted from a presently unidentified vent area to the south of the Landing. Armstrong and others (1975) comment on the extremely diverse ages and eruptive histories of Banbury-age basalts in this portion of the Snake River Plain. Much more work on these rocks is needed before definite correlations can be made.

Rhyolite Ash-Flow Tuffs of Magic Reservoir

The rhyolite ash-flow tuffs on the north side of Magic Reservoir are a multiple cooling unit comprised of several simple cooling units of quartz-sanidine rhyolite ash-flow tuffs. These rocks are exposed north, west and southwest of Hot Springs Landing, where they form a section as thick as 110 m. The section is much thinner southeast of the landing, measuring only 40 m thick and consisting of only one ash-flow unit.

The ash-flow tuffs of Magic Reservoir are described briefly by Malde and others (1963), and correspond to the Poison Creek Tuffs mapped by Schmidt (1961). However, in order to avoid confusion with the Poison Creek time-stratigraphic unit used by Armstrong and others (1975) to describe upper Miocene silicic volcanic rocks near Bruneau, Idaho, in this study these rocks will be referred to as the rhyolitic ash-flow tuffs of Magic Reservoir.

Tuff 1

The base of the ash-flow sequence at Magic Reservoir, Tuff 1, is a 40 m thick simple cooling unit composed of a quartz-sanidine rhyolite ash-flow tuff exposed north, south and west of Hot Springs Landing. The best exposure of the base of Tuff 1 occurs approximately 0.25 km west-northwest of the landing, where it is draped nonconformably upon a rounded knob of the older rhyolite. A 30 cm thick, white, glassy, nonwelded porous zone forms the base of Tuff 1. Immediately overlying this nonwelded base is a densely welded black vitrophyre containing approximately 5 percent sanidine and quartz

crystals. The basal vitrophyre grades into a densely welded, partially devitrified red and black banded, granular tuff, locally containing fiamme of black glass. Pumice fragments in this section show extreme flattening and compaction. This partially devitrified zone grades upwards into a thoroughly devitrified zone characterized by a stony pink rather than a black, glassy appearance. The devitrified zone is overlain by a section of pink and orange, partially to slightly welded crystal lapilli tuff with porous pumice fragments showing decreasing amounts of compaction towards the top of the unit. Vapor-phase crystallization is common in these pumice fragments. The top of Tuff 1 consists of a totally nonwelded grayish-pink crystal tuff containing about 5 percent crystals of quartz and sanidine and a trace of biotite. This zone is thoroughly devitrified with well-developed vapor-phase crystallization in the pumice fragments. A petrographic description of Tuff 1 is included in Table 1, and the chemical composition in Table 2.

On the southeastern side of the study area, Tuff 1 is about 40 m thick and forms inconspicuous ridges along the northwest portion of the Clay Bank Hills. The nonwelded base of Tuff 1 is not seen; the black vitrophyre is only locally exposed. As on the northern side, Tuff 1 overlies the older rhyolite. However, on the southeastern side, Tuff 1 also locally overlies flows of Square Mountain basalt where these basalts cover the older rhyolite. The partially welded and nonwelded portions of Tuff 1 are poorly exposed on the

southeastern side and resemble the equivalent zones described to the north.

Tuff 2

In the northern portion of the study area, Tuff 1 is overlain by a 20 m thick ash-flow unit, Tuff 2. The exposed base of Tuff 2 is a densely welded, partially devitrified, crystal lapilli ash-flow tuff containing black fiamme in a pinkish-gray groundmass. No underlying basal vitrophyre or porous nonwelded zones were observed. The middle zones of Tuff 2 become increasingly devitrified and less welded with increasing distance from the base. The top of the unit is a slightly welded lapilli crystal tuff with abundant vapor-phase crystallization of the porous pumice fragments. The pumice fragments are maroon and show very slight compaction; the groundmass is light pink. The phenocryst mineralogy is quite similar to Tuff 1, consisting of about 5 percent quartz and sanidine. Tuff 2 is absent from the southeastern portion of the map area.

Tuff 3

Tuff 3 is restricted to the northern part of the study area where it is approximately 50 m thick. Like the base of Tuff 2, the nonwelded base of Tuff 3 was not observed. However, Tuff 3 does have a well-developed vitrophyre near its base. This vitrophyre is similar to the vitrophyre at the base of Tuff 1 and consists of about 5 percent of sanidine and quartz grains in a matrix of black glass with minor rust-colored glassy bands. This vitrophyre grades upwards into a gray

to maroon, densely welded zone in which most megascopic pyroclastic features are obscured by devitrification. Spherulitic devitrification is common in Tuff 3 and is recognized in hand sample as well-developed lithophysae. Lithophysae are most abundant in the zone of partial welding where they measure up to 10 cm in diameter. This spherulitic devitrification is useful in distinguishing Tuff 3 from Tuffs 1 and 2. This zone has also undergone minor vapor-phase crystallization. The top of Tuff 3 is a slightly welded lapilli crystal tuff containing barely flattened pinkish-red pumice fragments in a salmon-pink groundmass. Lithophysae are absent from this zone; vapor-phase crystallization occurs in the pumice fragments. The phenocryst mineralogy and groundmass characteristics of this unit are discussed in Table 1, and Table 2 lists the chemical composition.

Pumice of Magic Reservoir

The pumice of Magic Reservoir overlies Tuff 3 in the northern part and Tuff 1 in the southeastern part of the map area. It is well exposed in prospect pits and outcrops north of Hot Springs Landing and in a quarry on the north side of Highway 68, about 1.2 km north-northwest of the landing (Figure 4). On the southeastern side of the study area, the pumice occurs only as float and is not mapped as a separate unit. The relationship between the pumice and Tuff 3 is unclear. The pumice probably represents a separate event from Tuff 3. However, it could also be the nonwelded top of Tuff 3.

This unit is a distinctive pale orange, poorly sorted pumice flow. Textural variations include pumiceous crystal tuff, pumiceous

crystal lapilli tuff, and agglomerate. The pumice contains about one percent crystals of quartz and sanidine with minor biotite and obsidian. The fragments range in size from 30 mm to 1 m and are identical in appearance to the surrounding tuff matrix. The pumice has a silky, vitreous luster and a filamentous texture. Exposed within the pumice unit in the quarry is a thin unit of air-fall tuff consisting of well-sorted, subround pumiceous lapilli identical to those described above.

Source Area for the Magic Reservoir Rhyolite Ash-Flow Tuffs

The source area for the Magic Reservoir ash-flow tuffs is unknown. The presently known areal distribution of these rocks is limited to the vicinity of Magic Reservoir (Rember and Bennett, 1979), suggesting a local source. The pumiceous agglomerate and air-fall tuff exposed in the quarry are characteristic of near-vent pyroclastic deposits. However, these rocks could be significantly younger than the Magic Reservoir ash-flow tuffs.

The extreme degree of welding in the Magic Reservoir ash-flow tuffs may also imply a nearby source. Dense welding is characteristic of either thick cooling units and/or high temperatures of emplacement (Smith, 1960; Ross and Smith, 1961). Because the individual cooling units at Magic Reservoir have a maximum thickness of only 50 m, the observed dense welding is probably due in large part to high temperature. Since the hottest portion of an ash-flow is likely to be close to the vent area, the inferred hot nature of the Magic Reservoir ash-flow tuffs may suggest a nearby source.

Schmidt (1961) speculates that Moonstone Mountain (Figure 4) is an eruptive center and the source of the Moonstone Rhyolite. Additional field work, age-dating and petrochemical study are needed to ascertain whether the Magic Reservoir ash-flow tuffs can be correlated with the Moonstone Rhyolite. K-Ar age relationships discussed below suggest that the Moonstone Rhyolite and the Magic Reservoir ash-flow tuffs are contemporaneous.

Rhyolite Dome

The rhyolite dome of Magic Reservoir crops out 200 m due north of the landing and along the waterfront west-northwest of the landing. This unit is best exposed in the massive cliffs 500 m west-northwest of the landing where it attains a maximum thickness of 60 m.

There are two textural varieties of this rhyolite. The most abundant type is a massive, vertically flow-banded rock. Large-scale vertical and concentric joints are developed parallel to the flow-banding. Erosion along these joints produces ravines, crags and spires. Flow-banding is continuous for several meters but is locally folded and contorted. The rock is light gray and contains approximately 5 percent fine-grained phenocrysts of quartz and sanidine. Much of the flow banding retains a slightly glassy luster and is darker-gray than the surrounding rock. This unit locally contains gas cavities and spherulites; minor vesiculation is common in the upper portions.

The second textural variety of this rhyolite, exposed near the

waterline 0.75 km west of the landing, is more coarsely crystalline and contains up to 15 percent phenocrysts of quartz, sanidine, biotite and magnetite. The phenocrysts in this phase are more altered than those in the fine-grained, banded portion. Iron-oxide staining fringes the mafic and opaque phenocrysts; the feldspars are partially altered. This portion of the unit occurs at the base and in the interior of the dome. More detailed descriptions of the rhyolite dome are included in Table 1 and the chemical composition is listed in Table 2.

The contact between the dome and the ash-flow tuffs is very sharp. The feeder zone of the dome cross-cuts the ash-flow tuffs at a high angle. This contact is well exposed 500 m west of Hot Springs Landing, a short distance above the water line. Locally the contact is a marginal friction-breccia (Williams and McBirney, 1979, p. 193) of angular ash-flow tuff fragments incorporated in the sides of the dome.

The steep, concentric joints, flow-banding, and rugged, spiny form of this rhyolite is characteristic of many silicic domes (Williams and McBirney, 1979, pp. 188-190). The glassy, flow-banded rhyolite occurs in the upper and exterior parts of the dome; the more coarsely crystalline variety is from the more slowly cooled base and interior. The breccia of ash-flow tuff fragments locally developed along the contact of the rhyolite dome with the ash-flow tuffs clearly demonstrates that the dome is younger than the ash-flows. K-Ar age relationships presented below verify this chronology. The breccia

also suggests that this represents a vent area which has been filled by the feeder zone of the rhyolite dome.

Quaternary Sediments, Sedimentary Rocks, and Basalts

Quaternary rocks are exposed throughout the study area. The Quaternary units include three sediments, one sedimentary rock and two basalts. These will be discussed in chronological order.

Myrtle Sediments

The oldest sedimentary unit in the area, the Myrtle Sediments (Schmidt, 1961), is a sequence of fluvial and lacustrine arkosic sediments best exposed in prominent bluffs along the west side of Magic Reservoir from Magic Resort to Hot Springs Landing (Figure 4). This sediment is also seen a short distance up Camas and Rock Creeks, and in one small area 900 m due south of Hot Springs Landing where this unit lapped onto a horst.

The Myrtle Sediments form a 17 m thick outcrop at the west side of Poison Creek inlet. It may be much thicker since a driller's log of a water well at Hot Springs Landing indicates the presence of 79 m of sand, gravel and shale. The base of these sediments is not exposed, even when the reservoir is near its lowest level. The upper contact of this sediment is a conformable, although irregular, surface with the Quaternary Macon Basalt. The load-deformed top of the sediments 800 m south-southwest of the landing displays 0.5 to 1 m interpenetrations with the base of the basalt.

This oldest sedimentary stratum is so poorly lithified that sedimentary structures are not generally discernable. Where sedimentary structures are seen, the thinly laminated to thinly

cross-laminated strata, together with the presence of oscillation ripple marks, suggest lacustrine sedimentation. This unit is comprised of both a subarkose and a subordinate amount of light gray-green shaley siltstone. The subarkose is medium- to very coarse-grained with scattered granitic and gneissic pebbles. It is poorly sorted with subangular to subrounded clasts, indicating rapid transportation and sedimentation from a nearby source area. The gray-green siltstone is best exposed along the west side of Poison Creek inlet where approximately 2 m of the siltstone are exposed when the reservoir is at low water level.

The Quaternary Basalts

Two flat-lying Quaternary basalt flows are mapped near Hot Springs Landing. Malde and others (1963) assign these flows to the Bruneau Formation. Armstrong and others (1975) report a K-Ar date of 0.8 m.y. for a Bruneau Basalt flow 10.5 km southwest of Hot Springs Landing. Schmidt (1961) assigns these basalts to the Bellevue Formation.

The two basalt flows are separated by a northwest-trending horst at Hot Springs Landing (Figure 3). Schmidt (1961) names the basalts southwest of the landing the Macon Member and the flows east of the landing the Wind Ridge Member. The basalts are distal tongues of flows which erupted from two widely spaced eruptive centers (Schmidt, 1961).

In the study area, the Macon Basalt only has one recognizable flow while the Wind Ridge Basalt has at least three flows, each 4 to 8 m thick. Otherwise, the two basalts are similar. The tops and bottoms of the flows are rubbly and vesicular. The interior portions display well-developed columnar jointing. On fresh surfaces, the basalt is medium- to dark-gray and has vesicles which are commonly filled with calcium carbonate. The rock is very fine-grained with local aggregates of feldspar, pyroxene, and altered, bronze olivine. See Table 1 for a petrographic description of the Quaternary basalts.

Macon Sediments

The second sedimentary unit, the Macon Sediments of Schmidt (1961), occurs at lower elevations throughout the study area and is up to 5 m thick. The unit is totally unlithified and forms no outcrops. It is present only as a veneer of loose sand, gravel and scattered cobbles. The base of the Macon Sediments is not prominently exposed but appears to be conformable where it overlies the Macon Basalt and the Myrtle Sediments. Otherwise, it is nonconformable with the older igneous units. The coarser clasts are dominantly gray orthoquartzite; the sand is arkosic. The Macon Sediments were largely deposited by Camas Creek, west of the Hot Springs Landing horst, and Rock Creek to the east.

Unnamed Quaternary Conglomerate

Unnamed Quaternary arkosic, silica-cemented conglomerates were recognized at four places in the study area. Along the east side of Poison Creek inlet (Figure 3) they form approximately 5 m thick

resistant ledges, unconformable with the underlying Tuff 1. This conglomerate contains clasts of Magic Reservoir Tuffs up to 30 cm long with smaller fragments of metasediments and granitic rocks. The conglomerate exhibits only the vaguest indications of bedding, and probably formed by a mixing of colluvium and Macon Sediments transported to the site by Poison Creek.

A variant of this conglomerate occurs 200 m N75°W of the landing and 500 m and 750 m west of the landing, on the south side of Camas Creek. Although similar to the conglomerate at Poison Creek, these three occurrences differ in having a greater proportion of locally derived tuff fragments, by having ferruginous and siliceous cement, and by exhibiting much smaller average clast size (10 cm maximum length). This ferruginous conglomerate is in close proximity to the major west-trending fault mapped along Camas Creek. The westernmost of these three outcrops is located along the western horst-bounding fault. The ferruginous and siliceous nature of this conglomerate, and its proximity to major faults in the area, suggest that the silica and iron cements may be from fluids of possible thermal origin.

Quaternary Alluvium

The youngest sediment present in the area is Quaternary alluvium. No detailed study was done of these sediments, but where seen they are obvious mixtures of the lithologies from their respective drainages.

STRUCTURE

The structure of the Magic Reservoir area (Figure 3) is dominated by extensional tectonics. High-angle normal faults displace all pre-Quaternary rock units and give the area a block-faulted configuration. Major faults trend west, northwest, and northeast. A west-trending series of linear features extending from the southwestern portion of the mapped area to the Camas Prairie to the west (Figure 4) is also observed.

A major west-trending fault parallels the east-west segment of the the Wood River east of Hot Springs Landing and Camas Creek west of the landing (Figure 4). This fault is mapped on the basis of stratigraphic offset and inferred from the presence of a prominent linear feature observed on aerial photographs. The south side of the fault has dropped relative to the north side. The amount of displacement is speculative because of the lack of a definitive marker horizon across the fault. Since the exposed thickness of Tuff 1 both north and south of the fault is the same, the base of Tuff 1 may represent a level, pre-ash flow depositional surface, and therefore would be a relatively good marker horizon. If so, then the south side has dropped 200 m relative to the north side.

Three minor west-trending faults are mapped in the area. Two are immediately north of Hot Springs Landing. The other is mapped in the Clay Bank Hills to the south. The displacement along these minor west-trending faults appears to be minimal, suggesting that they are

nearly vertical, tensional fractures. Where observed, the relative movement of these faults is south side down. These smaller faults are probably step faults which formed in response to displacement of the larger fault. The persistent northerly dips of the ash-flow tuffs observed throughout the study area might be explained in terms of slight rotation along the west-trending faults, forming a tilted, step fault block pattern. A similar mechanism is postulated for the structures observed in fault blocks of the Basin and Range province (Stewart, 1971).

In addition to the west-trending faults, high-angle northwest- and northeast-trending normal faults also cut the silicic volcanic rocks and the Square Mountain Basalt. The two fault sets bound a horst which will be referred to as the Hot Springs Landing horst. Because of the relatively continuous fault traces of these two sets of faults, they are believed to postdate the west-trending faults.

The northwest-trending faults are better exposed than the northeast-trending faults. As shown in Figure 3, a northwest-striking fault forms the prominent scarp along the west side of the Clay Bank Hills, isolates a small peninsula of ash-flow tuffs southwest of Hot Springs Landing, and forms the northwest-trending inlet of Poison Creek. Displacement is difficult to determine, but it is at least 150 m, the height of the Clay Bank Hills fault scarp. Roughly paralleling this to the northeast is a less conspicuous fault which is mapped on the basis of a 14 m offset in the ash-flow stratigraphy north of Hot Springs Landing.

A northeast-trending fault marks the boundary between the Magic Reservoir rhyolites and the Quaternary rocks east of Hot Springs Landing. Its southward extension is marked by a short linear scarp at the tip of the Clay Bank Hills. Continuation of the fault to the south beneath younger basalts and sediments is drawn on the basis of photo-linear interpretation. The amount of offset along this fault cannot be determined, but it is believed to be in excess of 95 m, based on topographic evidence.

The overall pattern produced by the northwest- and northeast-trending faults is a scissors-type arrangement in which the Clay Bank Hills and the ridge north of Hot Springs Landing are separate, V-shaped horsts. It is likely that this block faulting was established prior to emplacement of the Quaternary basalts and sediments which are flat lying, largely unfaulted, and limited in areal distribution by the horsts.

The west- and northwest-trending features in the Magic Reservoir area conform to the regional structural patterns in this part of the Snake River Plain. The west-trending faults and linear features near Magic Reservoir parallel the east-west structural grain defined by the physiography in Camas Prairie to the west and the Mount Bennett Hills to the southwest (Figure 4). Both are prominent east-west-trending features in the north-central portion of the Snake River Plain, although their structural development and age relative to other features of the Plain are unknown (Mitchell, 1976).

The northwest-striking faults coincide with the dominant regional structural grain mapped in the Mount Bennett Hills-Magic Reservoir area by Malde and others, (1963), Smith, (1966), and Mitchell (1976). A strong northwest-trending gravity anomaly just east of Hot Springs Landing (Mabey and others, 1974) parallels this northwest-trending fracture pattern. The high-angle, northwest-striking faults are believed to be the result of a tensional stress field which has existed for the last 5 m.y. in the north-central portion of the Snake River Plain (Furlong, 1979).

COMPARISON OF THE MAGIC RESERVOIR RHYOLITES TO OTHER NEARBY SILICIC VOLCANIC ROCKS

The rhyolites of Magic Reservoir differ mineralogically and chemically from the Idavada volcanics in the nearby eastern Mount Bennett Hills (Figure 4). The eastern Mount Bennett Hills Idavada sequence is comprised of a series of silicic ash-flow tuffs and minor intercalated basalts with an aggregate thickness of 457 m (Smith, 1966). These ash-flow tuffs are apparently less silica-rich than the units at Magic Reservoir. The SiO₂ content of the eastern Mount Bennett Hills Idavada volcanics ranges from 67 to 71 percent, as determined by Smith (1966) from measurements of refractive indices of fused glass samples from the welded portions of the tuffs. (Complete chemical analyses for these rocks are not available). The SiO₂ content of the Magic Reservoir rocks ranges from 70.54 to 76.77 percent as determined by ICP analysis (Table 1). In contrast to the sanidine-rich Magic Reservoir rhyolites, the feldspar phenocryst assemblage of the Idavada volcanics is composed mainly of plagioclase with minor sanidine (Smith, 1966). Additional work on the chemical composition of silicic volcanic rocks in the Snake River Plain is needed to ascertain whether there is significant chemical variation between the Magic Reservoir rhyolites and other Snake River Plain rhyolites.

The Moonstone Rhyolite exposed in the extreme eastern portion of the Mount Bennett Hills (Smith, 1966 and Schmidt, 1961), and at Moonstone Mountain (Schmidt, 1961) is mineralogically similar to the

older rhyolite. Moonstone Mountain is an endogenous rhyolite dome containing abundant phenocrysts of fresh sanidine, rounded-resorbed quartz, altered plagioclase, pigeonite, oxyhornblende and accessory magnetite, zircon, apatite and allanite (Schmidt, 1961). Schmidt (1961) states that a rhyolitic composition has been determined for the rocks of Moonstone Mountain, although a chemical analysis is not provided. The base of the dome is described by Schmidt (1961) as dark brown, dense, glassy and highly porphyritic. Reconnaissance field examination of the lobate flow extending southeast from the base of Moonstone Mountain reveals striking textural and mineralogical similarity between this unit and the older rhyolite of Magic Reservoir. In addition, the Moonstone Rhyolite is locally overlain by the Square Mountain Basalt, and thus occupies the same stratigraphic position as the older Magic Reservoir rhyolite in the southeastern part of the study area. On the basis of their stratigraphic position and mineralogical similarity, these two units are tentatively correlated with each other. Additional work is needed to verify this correlation.

Four silicic dome-like features occur southeast of Magic Reservoir (Figure 4). Reconnaissance field examination reveals these to be circular, funnel-shaped structures with well-developed flow layering, and steep, concentric jointing. Petrographic examination of the silicic lavas from Rattlesnake Butte, the northernmost dome-like structure (Figure 4), reveals many similarities to the more coarsely crystalline, interior portions of the rhyolite dome at Magic Reservoir.

REGIONAL VOLCANIC STRATIGRAPHY AND AGE RELATIONSHIPS
OF THE MAGIC RESERVOIR RHYOLITES

Three rhyolites from the Magic Reservoir study area were selected for K-Ar dating (Table 3). These newly reported ages suggest that silicic volcanism in the Magic Reservoir area spans the period between 5.98 ± 0.69 and 3.06 ± 0.04 m.y. The 3.06 m.y. date is obtained by Armstrong and others (1975) from Wedge Butte. On the basis of these dates, there appear to be two periods of silicic magmatism in the Magic Reservoir area. The earliest event, the Magic Reservoir event, occurred around 5.98 m.y. ago. This period includes both the older rhyolite and the ash-flow tuffs at Magic Reservoir. (Since the age dates for these rocks are statistically indistinguishable, they are considered the same event). The Magic Reservoir period is also inferred to include the Moonstone rhyolites based upon the tentative correlation between the Magic Reservoir older rhyolite and Moonstone rhyolite. This inferred age relationship lends support to the contention that Moonstone Mountain may be the source of the Magic Reservoir ash-flow tuffs.

The second period of silicic magmatism in the Magic Reservoir area is the 3.06 m.y. old Wedge Butte event. The available information presently limits this stage to Wedge Butte, since the ages of the three other nearby domes are unknown. The 4.94 m.y. old Magic Reservoir dome might be an earlier phase of this volcanism. However, the nearly identical ages and chemistry of the Magic Reservoir dome and ash-flow tuffs suggests that the dome probably represents the

waning stages of the Magic Reservoir event. In contrast to the explosive nature of the Magic Reservoir volcanism, no pyroclastic rocks have yet been identified with the Wedge Butte period.

REGIONAL SIGNIFICANCE OF THE MAGIC RESERVOIR RHYOLITES

Regional age-dating studies of silicic and basaltic volcanic rocks in the Snake River Plain (Armstrong and others, 1975, 1980) demonstrate that volcanism in the Snake River Plain migrates with time from west to east. The Idavada silicic volcanic sequence began about 15 m.y. ago in the western Snake River Plain, and about 5 m.y. ago in the eastern Snake River Plain. Although few caldera structures are known in the western Snake River Plain due to burial by younger basalts, the Idavada volcanics probably erupted from a series of nested or coalescing calderas. Subsidence along the axes of these coalescing calderas may, in part, form the axial downwarp of the Snake River Plain (Christiansen and Lipman, 1972; Suppe and others, 1975; and Prostka, 1975).

This phase of silicic volcanism is followed by dominantly basaltic volcanism which has filled and buried most of the caldera structures. Like the silicic volcanic event, basaltic volcanism is also time-transgressive, beginning about 10 m.y. ago in the western Snake River Plain and shifting eastward with time to its present position in the eastern Snake River Plain (Armstrong and others, 1975).

The rhyolites of the Magic Reservoir area do not fit well into this described pattern of eastward-transgressive silicic volcanism. The K-Ar dates for the Magic Reservoir rhyolites and for Wedge Butte are anomalously young when compared to the ages of nearby Idavada

volcanic rocks. For example, in the eastern Mount Bennett Hills, the base of the Idavada volcanics is 10.0 m.y. old. In the northern Mount Bennett Hills an 11.0 m.y. date is reported for an unidentified horizon in the Idavada sequence (Armstrong and others, 1980). Other silicic volcanic rocks in this portion of the Snake River Plain range in age from 6.25 m.y. at Shoshone Falls, east-northeast of Twin Falls, to 9.2 m.y. in the Malta Range, east-southeast of Twin Falls (Armstrong and others, 1975). These dates are shown in the time-space profile of Figure 5. On the basis of these age dates it is clear that the flows and pyroclastic rocks of Magic Reservoir should not be grouped with the Idavada volcanic rocks. The Magic Reservoir rhyolites are anomalously young and represent a local renewal of silicic volcanism. They are the youngest silicic volcanic rocks presently known this far west in the Snake River Plain.

The anomalously young age of the Magic Reservoir rhyolites can perhaps be best understood when placed within the regional framework of time-transgressive volcanism in the Snake River Plain. Although Figure 5 reveals that initiation of silicic and basaltic volcanism in the western Snake River Plain predates the initiation in the eastern Snake River Plain, there are abundant examples of contemporaneous, Holocene basalts throughout the Snake River Plain. The presence of Holocene basalts in the western Snake River Plain suggests that it is the inception of volcanism and not the termination of volcanism that migrates with time. Once volcanism has commenced in an area, it may persist. The Magic Reservoir rhyolites represent a unique example of

persistent silicic volcanism in the western Snake River Plain. Possible analogs of persistent, anomalously young silicic volcanism in the eastern Snake River Plain might include the 0.08 m.y. old China Hat rhyolite dome east of Pocatello or the 0.3 m.y. old rhyolites (Armstrong and others, 1975) at Big Southern Butte west-southwest of Idaho Falls (Figure 5).

The wide range of ages of silicic volcanic rocks in this portion of the Snake River Plain could also be due to the stratigraphic complexity of the Idavada Volcanics. The space-time profile of Figure 5 is probably overly simplified (W. P. Leeman, 1981, verbal communication), since the stratigraphy of the Idavada Volcanics is largely unknown. It is thus unclear whether the dates for Idavada rocks from one location can be meaningfully compared to dates from a different location. Divergent dates could represent, in part, different stratigraphic positions within the Idavada volcanic sequence. With this in mind, it would be useful to obtain a date from the top of the Idavada volcanic rocks in the eastern Mount Bennett Hills for comparison with the age of the Magic Reservoir event.

GEOHERMAL GEOLOGY OF THE MAGIC RESERVOIR AREA

The geothermal resource at Hot Springs Landing presently consists of a 79 m well that produces 57 l/min of 71°C (160°F) water (Mitchell and others, 1980). This well was drilled at the former site of Magic Reservoir Hot Springs. As a result of this drilling activity, the hot springs dried up. The hot springs had a reported temperature of 36°C (100°F) and a flow rate of 492 l/min (Ross, 1971). The ferruginous, silica-cemented sediments west and northwest of the landing may be an additional manifestation of the geothermal system. Fluid samples from the geothermal well yield a mean geothermometer estimate of reservoir temperature at depth of 149°C (300°F) (Muffler, 1979).

Like many of the geothermal resources in the Snake River Plain, the Magic Reservoir system is associated with normal faults. The system probably derives its heat from deep circulation of fluids along fractures. Fluids become heated at depth by conduction of heat from the rocks. Heated fluids may rise due to thermal expansion and become part of a hydrothermal convective cell as shown in Figure 6. Where favorable permeable structures like fault zones intersect this convective cell, the geothermal fluids may rise to the surface, forming hot springs. The area immediately surrounding the zone of upward-flowing water will have an elevated geothermal gradient due to the local convection of hot water. This convective gradient and associated heat flow anomaly are commonly limited in areal extent and should not be extrapolated to depth, or to areas removed from the immediate hot spring vicinity. Isothermal zones may occur along the

fault in systems with rapid upward convective flow (Figure 6).

There are numerous faults near Magic Reservoir which might serve as suitable geothermal fluid conduits. The intersection of the southeastern corner of the Magic Reservoir horst with the fractures trending north-northeast and west is immediately east-southeast of the landing. Fault intersections commonly play a role in localizing geothermal systems due to the enhancement of fracture-induced permeability. As suggested by Mitchell (1976), the hot springs present prior to the drilling of the Hot Springs Landing well may have been controlled by the intersection of these fracture zones. Since northwest-trending structures are dominant on both a local and a regional scale, the northwest-trending fractures may play the most important role in controlling the circulation of geothermal fluids.

Geothermometers (Fournier and others, 1974) are commonly used indicators of equilibrium temperature at depth. When coupled with nearby conductive geothermal gradient data, the minimum depth of circulation necessary to attain a geothermometer-predicted temperature can be estimated. The flowing geothermal well reflects a convective geothermal gradient and is not representative of the background conductive gradient (Figure 6). Unfortunately, there are no geothermal gradient data available from the immediate vicinity of Magic Reservoir. The nearest available conductive geothermal gradient is 60°C/km measured in a 52 m well at T2S, R20E, Sec. 21 about 28 km east-southeast of Hot Springs Landing (Brott and others, 1976). Extrapolating this conductive gradient to the Magic Reservoir area,

and assuming a yearly average shallow groundwater temperature of 15°C, implies that the Magic Reservoir fluids must circulate to a minimum depth of 2.2 km to attain a temperature of 149°C, the mean geothermometer estimate of reservoir temperature. Mitchell (1976) predicts a similar depth to the geothermal reservoir. Due to the slow and inefficient transfer of heat from rocks to water, fluids must probably circulate much deeper to reach this temperature. In zones of upward flow of geothermal fluids, 149°C water might be found at significantly shallower depths due to the upward-bowing of isotherms along zones of enhanced permeability and rapid convective flow, as shown in Figure 6. Such a zone of anomalous fluid temperature and fluid flow would be the target of a geothermal exploration program in the Magic Reservoir area.

The presence of young silicic volcanic rocks in the area does not suggest a molten or partially molten magma body at depth acting as a heat source for the Magic Reservoir system. As Figure 7 indicates, Smith and Shaw (1975, 1979) show that magma bodies with volumes between 1 and 10 km³ lose a significant amount of their magmatic heat and reach ambient temperatures at the depth of emplacement within 10⁵ years after eruption. The age of the silicic volcanic rocks in the Magic Reservoir area implies that the system would have to be on the order of 10³ km³ in order to retain any magmatic heat. There is no evidence presently available to suggest that the volcanic system is this large. Assuming an approximate volume of 3 km³ for the Magic Reservoir system based upon the presently known areal distribution of

about 20 km² and an average thickness of 150 m, and assuming that the erupted volume corresponds to the volume of the remaining magma chamber (Smith and Shaw, 1979), the inferred 3 km³ Magic Reservoir magma body would cool to 300°C in the center within 10⁴ to 10⁵ years after eruption (Figure 7). A more accurate estimate of the volume of the Magic Reservoir system cannot be made since the source area for these rocks is unknown. However, even if the distribution of the Magic Reservoir volcanic rocks is broadened to include the Wedge Butte event, the other undated domes southeast of Hot Springs Landing, and the southwestern extension of the Moonstone Rhyolite (Schmidt, 1961; Smith, 1966), the system is still too small to be molten. It is thus apparent that the heat flow observed at Magic Reservoir is due to the regional conductive heat flow and is not augmented by any latent magmatic heat.

The 0.8 m.y. old Bruneau basalt 10.5 km southeast of Hot Springs Landing (Armstrong and others, 1975), and the younger but undated Shoshone basalts south of the landing (Malde and others, 1963) are examples of the widespread recent basaltic volcanism common throughout much of the Snake River Plain, suggesting that the area is still an active basaltic magmatic province. However, like the silicic volcanic rocks, these basalts probably have insufficient volume to act as sources of magmatic heat. The conditions that may give rise to basalt formation, such as partial melting in the mantle due to elevated mantle temperatures, may enhance the regional conductive geothermal gradient and heat flow.

Despite the absence of a magmatic heat source, this area of Idaho has high heat flow. The average heat flow for the western Snake River Plain ranges from 1.7 HFU in the center and up to 3.0 HFU along the margins, compared to the average continental crustal heat flow of 1.5 HFU for the stable interior of the North American Plate (Brott and others, 1976). Recent gravity modeling of the western Snake River Plain (Mabey, 1976) reveals that this area has an anomalously thin upper crust. This thinned crust may provide less insulation than crust of normal thickness to heat flux from the mantle below, resulting in the observed elevated thermal regime. Areas of high heat flow are commonly associated with zones of thin crust (Condie, 1976, p. 60).

The position of the Magic Reservoir system along the northern border of the Snake River Plain, adjacent to the Idaho batholith, may also contribute to the elevated heat flow of the area. The southern and northern margins of the western Snake River Plain are areas of anomalously high heat flow compared to the interior of the western Snake River Plain. Brott and others (1978) attribute this enhanced heat flow to refraction of heat from high-conductivity granitic rocks of the Idaho batholith in contact with the lower-conductivity sedimentary and volcanic rocks of the Snake River Plain.

SUMMARY AND SUGGESTIONS FOR ADDITIONAL WORK

The source or sources of the ash-flow tuffs in the western Snake River Plain is largely unknown. Although these rocks probably erupted from a series of calderas (Christiansen and Lipman, 1972; Suppe and others, 1975; and Prostka, 1975), very few calderas are presently recognized.

Additional geologic mapping, petrochemical study and radiometric dating of the silicic volcanic rocks in the Magic Reservoir-Mount Bennett Hills area could help unravel the eruptive history of this portion of the Snake River Plain. The regional stratigraphic and age relationships of the Magic Reservoir rhyolites to other nearby silicic volcanic rocks should be determined. In particular, the correlation proposed in this study between the Magic Reservoir rhyolites and the Moonstone rhyolites should be tested. The top of the Idavada Volcanics in the eastern Mount Bennett Hills should be dated for comparison to the Moonstone and Magic Reservoir rhyolites. The age of the pumice at Magic Reservoir should be obtained in order to date the youngest, local pyroclastic event. The three undated domes southeast of the Landing should be studied to see whether they correlate with Wedge Butte or are closer in age to the dome at Magic Reservoir. Additional study of the distribution, age relationships and petrochemical affinity of these rocks may identify their eruptive source or sources and refine our understanding of the volcanic history of the western Snake River Plain.

The geothermal system at Magic Reservoir is controlled by deep circulation of fluids along fractures. The system probably does not derive any heat from the silicic volcanic rocks in the area since they are apparently too old to be associated with a molten or partially molten magma body. Thermal gradient drilling and testing are needed to evaluate further the geothermal potential of the area.

ACKNOWLEDGEMENTS

This study was performed under the User Assistance Program at the Earth Science Laboratory/University of Utah Research Institute. Funding was provided by the U.S. Department of Energy/Division of Geothermal Energy under contract number DE-AC07-80ID12079. The authors wish to thank D. Foley, J. Moore, D. Nielson, J. Stringfellow and E. Struhsacker for reviewing this paper, K. Wallwork and G. Mitoff for typing the manuscript, and K. Thompson and D. Cullen for drafting the figures.

REFERENCES CITED

- Armstrong, R. L., Leeman, W. P., and Malde, H. E., 1975, K-Ar dating, Quaternary and Neogene volcanic rocks of the Snake River Plain, Idaho: *American Journal of Science*, v. 275, p. 225-251.
- Armstrong, R. L., Harakal, J. E., and Neill, W. M., 1980, K-Ar dating of Snake River Plain (Idaho) volcanic rocks - new results: *Isochron/West.*, no. 27, p. 5-10.
- Brott, C. A., Blackwell, D. D., and Mitchell, J. C., 1976, Geothermal investigations in Idaho, Part 8, Heat flow study of the Snake River Plain, Idaho: Idaho Department of Water Resources Water Information Bulletin 30, 195 p.
- , 1978, Tectonic implications of the heat flow of the western Snake River Plain: *Geological Society of American Bulletin*, v. 89, p. 1697-1705.
- Christiansen, R. L., and Lipman, P. W., 1972, Cenozoic volcanism and plate-tectonic evolution of the western United States - Part II, Late Cenozoic: *Royal Society of London Philosophical Transactions*, ser. A., v. 271, p. 249-284.
- Condie, K. C., 1976, Plate tectonics and crustal evolution: New York, Pergamon Press, Inc., 288 p.
- Dalrymple, G. B., and Lanphere, M. A., 1969, Potassium-argon dating: W. H. Freeman and Company, San Francisco, 250 p.
- Fournier, R. O., White, D. E., and Truesdell, A. H., 1974, Geochemical indicators of subsurface temperature - part 1, basic assumptions: *U.S. Geological Survey Journal of Research*, v. 2, no. 3, p. 259-262.
- Furlong, K. P., 1979, An analytic stress model applied to the Snake River Plain (northern Basin and Range province, U.S.A.): *Tectonophysics*, v. 58, p. 11-15.
- Leeman, W. P., and Manton, W. I., 1971, Strontium isotopic composition of basaltic lavas from the Snake River Plain, southern Idaho: *Earth and Planetary Science Letters*, v. 11, p. 420-434.
- Mabey, D. R., 1976, Interpretation of a gravity profile across the western Snake River Plain, Idaho: *Geology*, v. 4., p. 53-55.
- Mabey, D. R., Peterson, D. L., and Wilson, L. W., 1974, Preliminary gravity map of southern Idaho: *U.S. Geological Survey Open-File Report 74-78*.

- Malde, H. E., Powers, H. A., and Marshall, C. H., 1963, Reconnaissance geologic map of west-central Snake River Plain, Idaho: U.S. Geological Survey Miscellaneous Geologic Investigations, Map I-373, scale 1:125,000.
- Mitchell, J. C., 1976, Geothermal investigations in Idaho, Part 7, Geochemistry and geologic setting of the thermal waters of the Camas Prairie area, Blaine and Camas counties, Idaho: Idaho Department of Water Resources Water Information Bulletin 30, 44 p.
- Mitchell, J. C., Johnson, L. L., and Anderson, J. E., 1980, Geothermal investigations in Idaho, Part 9, Potential for direct heat application of geothermal resources: Idaho Department of Water Resources Water Information Bulletin 30, 396 p.
- Muffler, L. J. P., ed., 1979, Assessment of geothermal resources of the United States - 1978: U.S. Geological Survey Circular 790, 163 p.
- Prostka, H. J., 1975, Structure and origin of the eastern Snake River Plain, Idaho [abs.]: Geological Society of America Abstracts with Programs, v. 7, no. 5, p. 637.
- Rember, W. C., and Bennett, E. H., 1979, Geologic map of the Hailey quadrangle, Idaho: Idaho Bureau of Mines and Geology, Geologic Map Series, Hailey 2° quadrangle.
- Ross, C. S., and Smith, R. L., 1961, Ash-flow tuffs: Their origin, geologic relations and identification: U.S. Geological Survey Professional Paper 366, 81 p.
- Ross, S. H., 1971, Geothermal potential of Idaho: Idaho Bureau of Mines and Geology, Pamphlet 150, 72 p.
- Schmidt, D. L., 1961, Quaternary geology of the Bellevue area in Blaine and Camas counties, Idaho [Ph.D. thesis]: University of Washington, 135 p.
- Smith, C. L., 1966, Geology of eastern Mount Bennett Hills, Camas, Gooding and Lincoln counties, Idaho [Ph.D. thesis]: University of Idaho, 170 p.
- Smith, R. L., 1960, Zones and zonal variations in welded ash-flows: U.S. Geological Survey Professional Paper 354-F, p. F149-F159.
- Smith, R. L., and Shaw, H. R., 1975, Igneous-related geothermal systems, *in* White, D. E., and Williams, D. L., eds., Assessment of geothermal resources of the United States - 1975: U.S. Geological Survey Circular 726, p. 58-83.

- _____, 1979, Igneous-related geothermal systems, in Muffler, L. J. P., ed., Assessment of geothermal resources of the United States - 1978: U.S. Geological Survey Circular 790, p. 12-17.
- Stewart, J. H., 1971, Basin and Range structure: A system of horsts and grabens produced by deep-seated extension: Geological Society of America Bulletin, v. 82, p. 1019-1044.
- Suhr, N. H., and Ingamells, C. O., 1966, Solution technique for analysis of silicates: Analytical Chemistry, v. 38, p. 730-734.
- Suppe, J., Powell, C., and Berry, R., 1975, Regional topography, seismicity, Quaternary volcanism, and the present day tectonics of the western United States: American Journal of Science, v. 275-A, p. 397-436.
- Williams, H., and McBirney, A. R., 1979, Volcanology: San Francisco, Freeman, Cooper & Co., 397 p.
- Wilson, W. R., and Chapman, D. S., 1980: Three topical reports: I. Thermal studies at Roosevelt Hot Springs, Utah; II. Heat flow above an arbitrary dipping plane of heat sources; III. A datum correction for heat flow measurements made on an arbitrary surface: University of Utah Report, DOE/ID/12079-19, 144 p.

<u>Rock Unit</u>	<u>Phenocryst Mineralogy</u>	<u>Groundmass Characteristics</u>
The Dider Rhyolite	This rock is comprised of 10 to 15% sanidine and anorthoclase laths, 10 to 15% subround quartz, 5% anhedral ferroaugite, lesser amounts of plagioclase, biotite, and opaque minerals, and accessory zircon and apatite. It also contains coarse-grained xenocrysts of microcline and plagioclase occurring as glomeroporphyritic clots associated with pyroxene and opaque minerals. The ferroaugite is altered in the devitrified portions of this unit to a fine-grained intergrowth of biotite, iron-oxide, chlorite and serpentine.	The groundmass ranges from glassy to totally devitrified. The glassy portions are a hypocrySTALLINE mixture of massive, nondevitrified glass, sparse patches of devitrified glass and tiny microlites. The devitrified variety is comprised mainly of patches of devitrified glass and microlites.
Square Mountain Basalt	This is a quartz-bearing basalt containing phenocrysts of plagioclase (An ₅₅), glomeroporphyritic clots of 0.5 to 1.5 mm long plagioclase and minor pale-green augite and pigeonite, coarse-grained xenocrysts of plagioclase and microcline with a uniform "swiss-cheese texture", and sparse, 1 to 2 mm embayed quartz xenocrysts.	The groundmass is comprised of plagioclase, opaque minerals, dark-brown interstitial glass and pyroxene microlites. This basalt has an intergranular texture.
Tuffs 1 and 2	These tuffs consist of a uniform phenocryst assemblage of 5 to 10% subhedral sanidine and anorthoclase, up to 1.0 mm in length, subround quartz ranging from 0.50 to 0.75 mm, minor plagioclase, biotite locally intergrown with chlorite and opaque minerals, and traces of apatite and zircon. These units also contain isolated grains and glomeroporphyritic clots of microcline, plagioclase associated with epidote and sericite, granophyric intergrowths of quartz and alkali feldspar, and moderately embayed quartz grains. The basal vitrophyre of Tuff 1 locally contains xenoliths of intergranular, augite-bearing basalt.	The basal vitrophyre of Tuff 1 is a nearly homogeneous black glass almost entirely lacking recognizable shard structures. All pumice fragments are completely collapsed and distorted, forming bands that resemble flow lines. Devitrification is minor; perlitic cracks are common. This vitrophyre resembles the zone of homogenization discussed by Smith (1960, p. 155) in which all pumice fragments, shards and glass dust are homogenized into a uniform glass. As welding decreases, the pumice fragments retain some of their original pore space. Vapor-phase crystallization becomes increasingly common in the porous pumice fragments in the partially welded to nonwelded portions of Tuff 1, and in small gas cavities within the groundmass. Devitrification is characterized by felty, radial, axiolytic and spherulitic intergrowths of alkali feldspar and cristobalite.
Tuff 3	Tuff 3 contains 5% phenocrysts of subround quartz, subhedral sanidine and anorthoclase, and minor plagioclase, hypersthene and opaque minerals. Hypersthene is altered to chlorite in the devitrified portions of this unit. The xenocryst content and mineralogy is similar to Tuff 1; no basaltic xenoliths were observed.	Except for the glassy, basal vitrophyre, this unit is characterized by abundant spherulitic devitrification. Spherulites consist of concentric bands of fine-grained intergrowths of cristobalite and alkali feldspar, exhibiting well-developed radial extinction. Vapor-phase crystallization is locally developed in gas cavities. Pumice fragments are recognizable throughout the unit. Glass shards, however, are difficult to identify due perhaps to their obliteration by extreme welding and/or devitrification.
The Rhyolite Dome	The flow-banded rhyolite contains 5 to 7% phenocrysts of fine-grained quartz, sanidine and anorthoclase, lesser amounts of plagioclase (An ₂₂₋₂₄) and opaque minerals, minor biotite and orthopyroxene, and accessory zircon and apatite. The orthopyroxene commonly occurs in glomeroporphyritic clots with opaque minerals and biotite, and is altered to a fine-grained intergrowth of biotite, chlorite and iron-oxide pseudomorphs after pyroxene. The coarsely crystalline portions of the dome contain 15 to 20% phenocrysts with the same mineralogy as the flow-banded rhyolite. The phenocrysts are more altered than in the flow-banded rhyolite. The feldspar phenocrysts are partially altered to sericite and epidote, the mafic phenocryst clots are extremely corroded and altered.	The groundmass of the flow-banded rhyolite is largely devitrified, consisting mainly of spherulites, exhibiting radial extinction. The flow-banding is faintly preserved in spite of the pervasive devitrification. Some of the flow bands remain glassy and reveal flowage around phenocrysts. The groundmass of the crystalline part of the dome is a cryptocrystalline intergrowth of quartz and feldspar.
Quaternary Basalts	The Quaternary basalts have an ophitic texture, and are comprised of 1 mm augite grains enclosing 0.1 to 0.2 mm labradorite (An ₅₇₋₆₇) laths, and glomeroporphyritic aggregates of labradorite, augite and minor olivine. The labradorite phenocrysts are acicular and radiate from a common point. Altered olivine and fresh augite occupy the interstices of the radiating feldspars.	The groundmass consists of plagioclase and pyroxene microlites, abundant disseminated opaque minerals and interstitial glass.

TABLE 4.
 PETROGRAPHIC DESCRIPTION
 OF THE RHYOLITES AND
 BASALTS AT MALLIC

TABLE 2.
CHEMICAL COMPOSITION
OF MAGIC RESERVOIR
AND OTHER SNAKE
RIVER PLAIN RHYOLITES

	Tuff 1		Tuff 3	Dome		Older Rhyolite**		Other Snake River Plain Rhyolites		
	ID/BE-10c	ID/BE-6	ID/BE-12A	ID/BE-106	ID/BE-21A	ID/MR-6	ID/BE-115	Idavada Composite++	Moonstone Mountain\$\$	Wedge Butte\$\$
SiO ₂	73.54	75.03	74.59	76.77	76.22	74.93	70.54	74.55	74.31	74.67
TiO ₂	0.24	0.22	0.22	0.24	0.21	0.31	0.64	0.39	0.23	0.10
Al ₂ O ₃	11.34	11.64	11.44	11.73	11.58	12.46	12.47	12.80	12.61	12.57
#Fe ₂ O ₃	2.11	2.00	2.03	2.18	1.93	2.34	4.92	1.63	2.20	1.53
FeO	0.82	0.44	0.26
MnO	0.03	0.02	0.03	0.03	0.01	0.01	0.05	0.04	0.049	0.034
MgO	0.25	0.16	0.17	0.22	0.11	0.17	0.42	0.22	0.09	0.02
CaO	0.83	0.66	0.62	0.61	0.51	0.75	1.81	1.03	0.83	0.70
Na ₂ O	2.42	2.98	2.96	2.85	2.79	3.14	2.93	3.06	3.34	3.94
K ₂ O	5.86	5.41	5.47	5.69	5.60	5.60	5.33	5.42	5.17	4.91
P ₂ O ₅	0.03	0.04	0.04	0.05	0.30	0.04	0.20	0.05	0.04	0.14
LOI	2.88	0.83	0.72	1.11	0.95	1.37	1.83
Oxide Total	99.53	98.99	98.29	101.48	100.21	101.12	101.14	100.01	99.31	98.87
Ba(ppm)	689	689	710	728	625	1,177	2,078
Zr(ppm)	272	276	274	274	267	388	697
†Sr(ppm)	58	50	50	51	49	106	188
†Be(ppm)	6.1	6.4	6.2	5.8	6.4	4.3	3.6
§Li(ppm)	32	42	43	19	42	28	20

*All analyses determined by lithium metaborate fusion ICP spectrographic techniques unless otherwise noted.

†Analysis determined by acid digestion ICP spectrographic technique.

§Lithium analyses determined by atomic absorption.

#Total Fe calculated as Fe₂O₃ for Magic Reservoir rhyolites.

**The variability in these two analyses is probably due to alteration. ID/MR-6 is somewhat altered; ID/BE-115 is glassy and fresh.

††Leeman and Manton (1971).

§§W. P. Leeman, 1981, written communication.

TABLE 3.
K-AR DATES AND
ANALYTICAL DATA
for the MAGIC RESERVOIR
RHYOLITES

Sample No.	Unit	Material Dated	Weight (gm)	%K	$^{40}\text{Ar}_{\text{Rad}} (\times 10^{11})$ (Moles/gm)	% $^{40}\text{Ar}_{\text{atm}}$	Age (m.y.)
ID/BE-21A	Dome	Sanidine	0.20200	6.06	5.203	75	4.94 ± 0.29
ID/BE-10C	Tuff 1	Anorthoclase	0.21614	7.70	7.823	53	5.85 ± 0.23
ID/BE-115	Older Rhyolite	Anorthoclase	0.21061	4.49	4.666	88	5.98 ± 0.69

Constants Used:

$$\lambda_{\beta} = 4.962 \times 10^{-10}/\text{yr.}$$

$$\lambda_{\epsilon} = 0.581 \times 10^{-10}/\text{yr.}$$

$$^{40}\text{K}/\text{K}_{\text{Tot.}} = 1.167 \times 10^{-4} \text{ Mole/Mole}$$

Potassium analyses done by lithium metaborate fusion technique of Subir and Ingamells (1966).

Argon analyses used standard isotope dilution techniques slightly modified from those of Dalrymple and Lanphere (1969).

Error limits to one standard deviation.

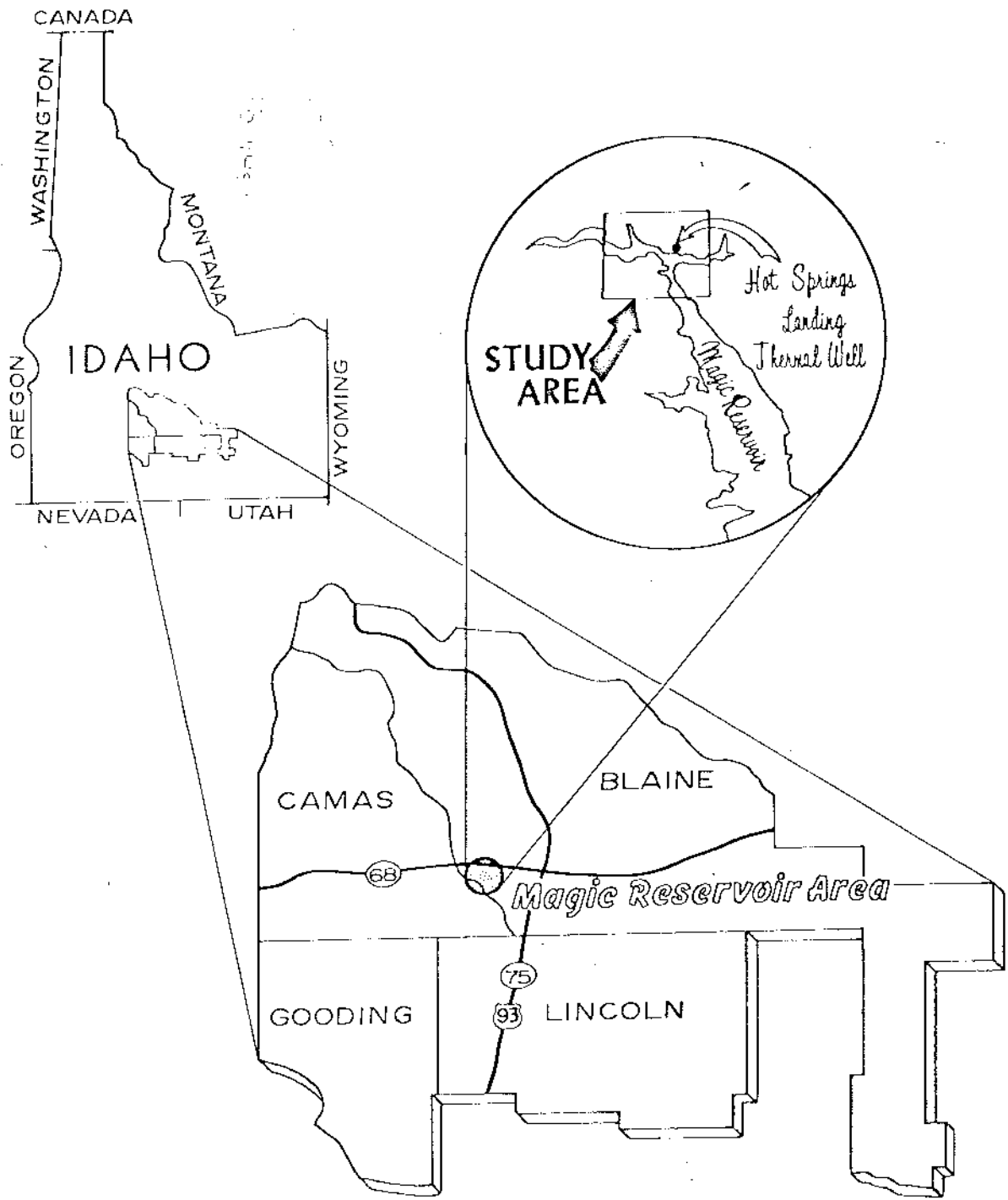


FIGURE 2
Index Map of the
Magic Reservoir Area

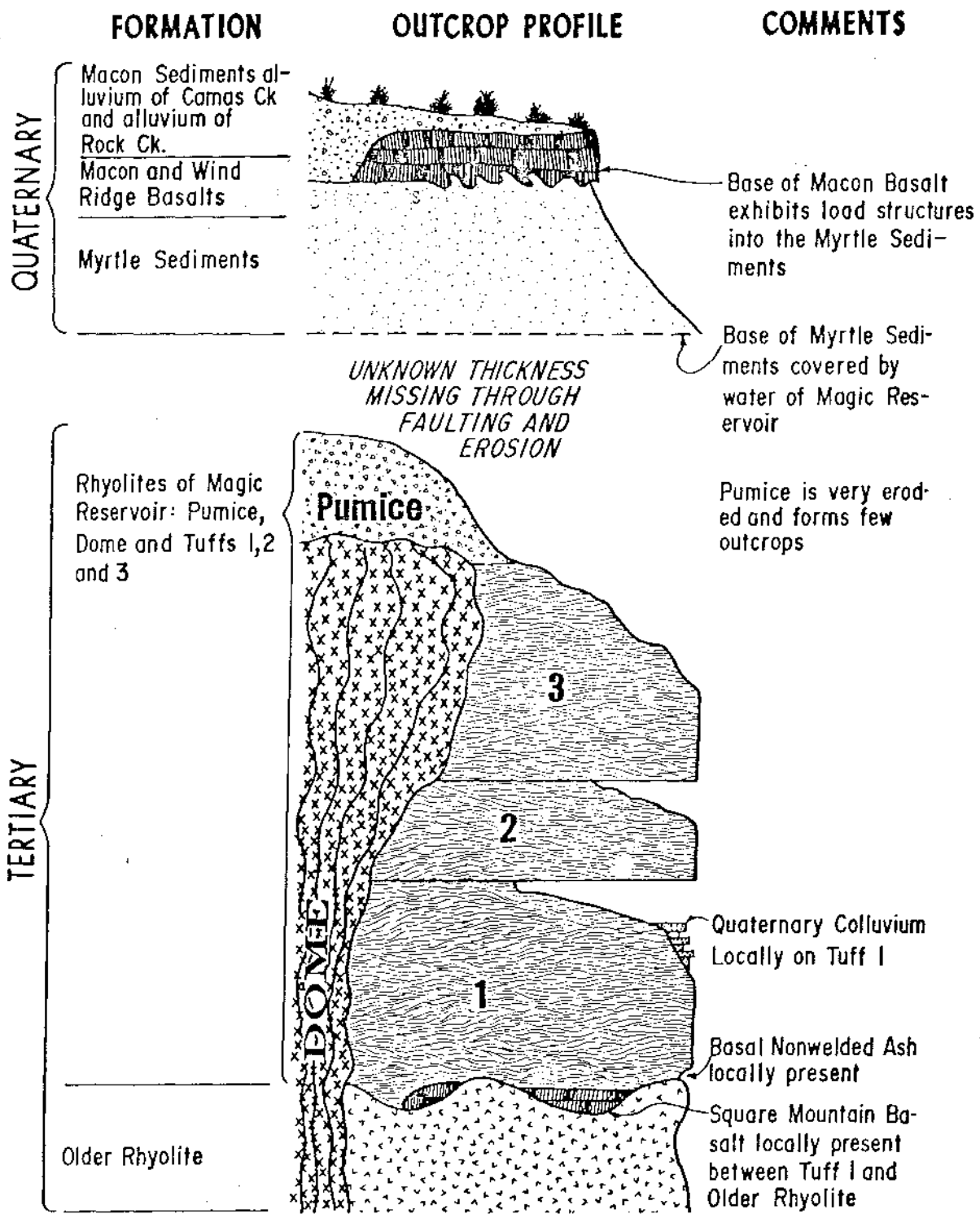


FIGURE 2
 DIAGRAMMATIC
 STRATIGRAPHIC COLUMN
 FOR THE MAGIC RESER-
 VOIR AREA

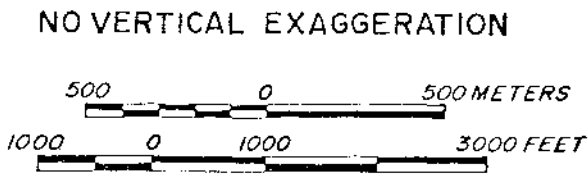
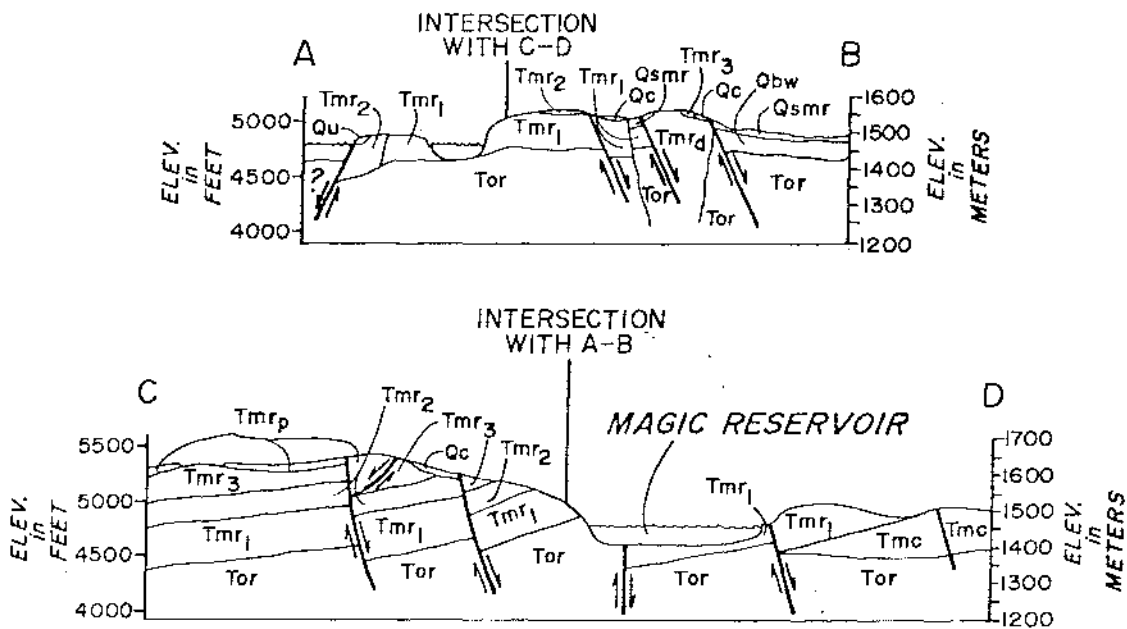
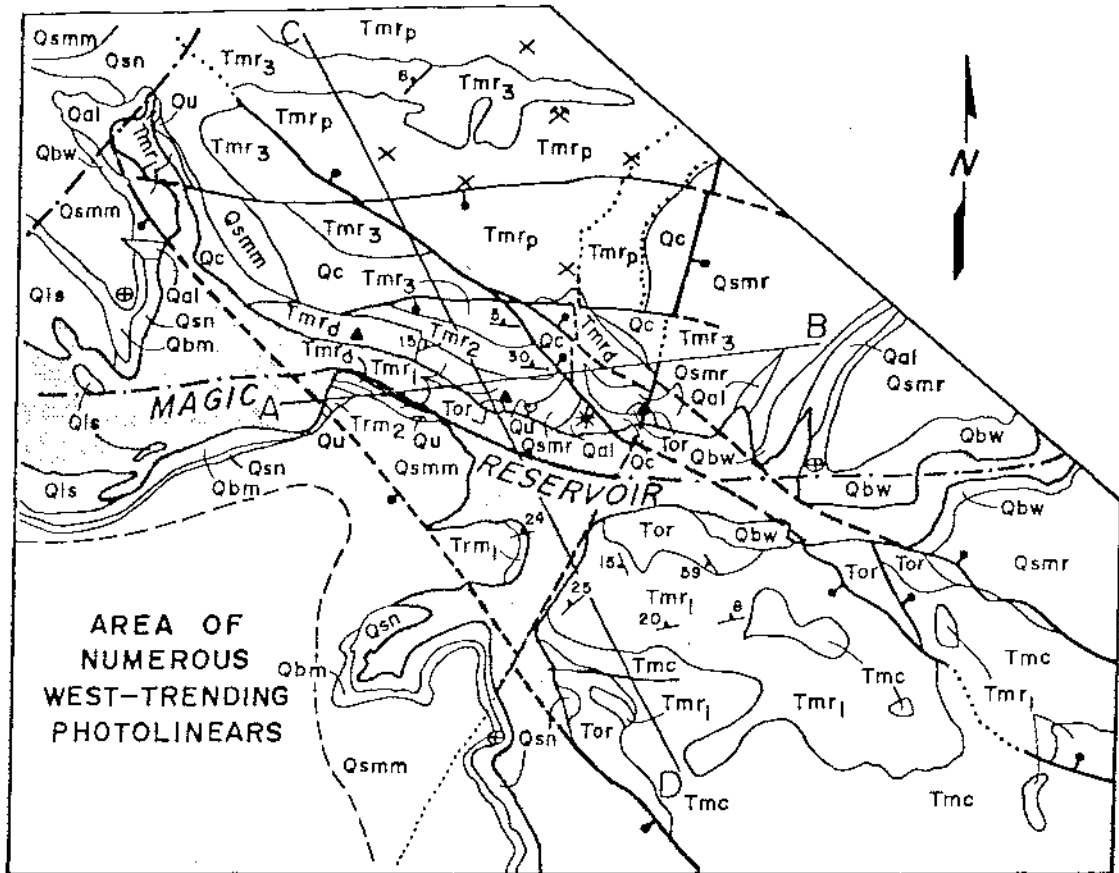


FIGURE 3.
GEOLOGIC MAP
AND CROSS SECTIONS
OF THE MAGIC
RESERVOIR AREA

MAP UNITS

- QUATERNARY
- Qls- Large-scale slump deposits
 - Qc- Colluvium
 - Qal- Alluvium
 - Qu- Unnamed Arkosic conglomerate
 - Qsmm- Macon Sediments derived from Camas Creek
 - Qsmr- Macon Sediments derived from Rock Creek
 - Qbm- Macon Basalt
 - Qbw- Wind Ridge Basalt
 - Qsn- Myrtle Sediments
- PLIOCENE
- Tmr_d - Rhyolite dome of Magic Reservoir (4.94±0.29m.y.)
 - Tmr_p - Pumice of Magic Reservoir
 - Tmr₃ - Tuff 3 of Magic Reservoir
 - Tmr₂ - Tuff 2 of Magic Reservoir
 - Tmr₁ - Tuff 1 of Magic Reservoir (..... ± m.y.)
 - Tmc- Square Mountain Basalt
 - Tor- Older Rhyolite of Magic Reservoir (5.98±0.69m.y.)

EXPLANATION


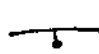
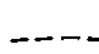
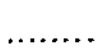
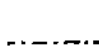


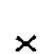



-  Contact
-  Mapped Fault—Ball on downthrown side
-  Inferred Fault
-  Photo interpreted extension of mapped fault
-  Photo-linear
-  Strike and dip of compaction foliation
-  Horizontal bedding
-  Prospect pit
-  Quarry
-  Age dating sample location
-  Hot Springs Landing Thermal Well

FIGURE 4.

PHYSIOGRAPHIC MAP
OF THE MAGIC
RESERVOIR REGION

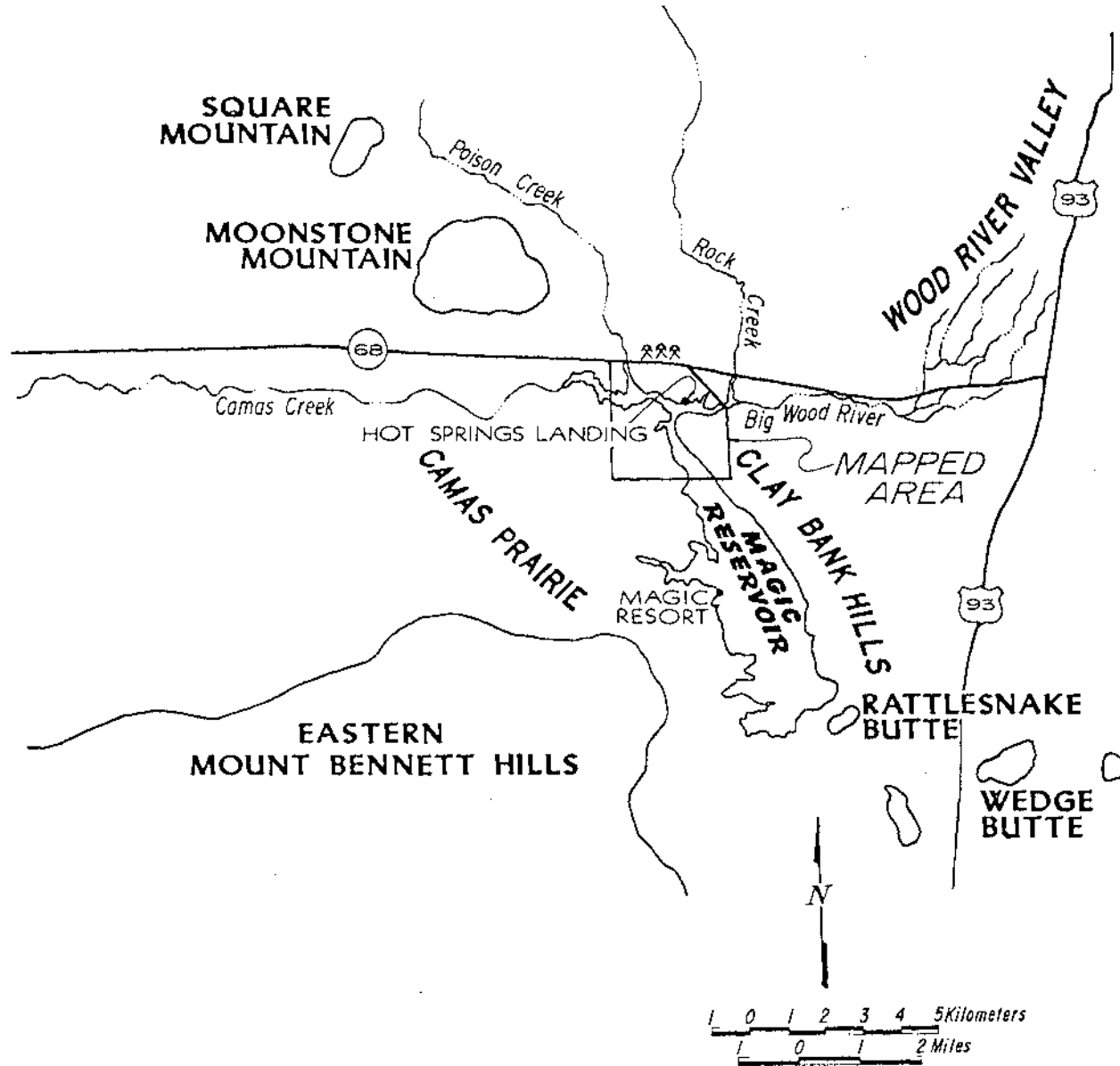
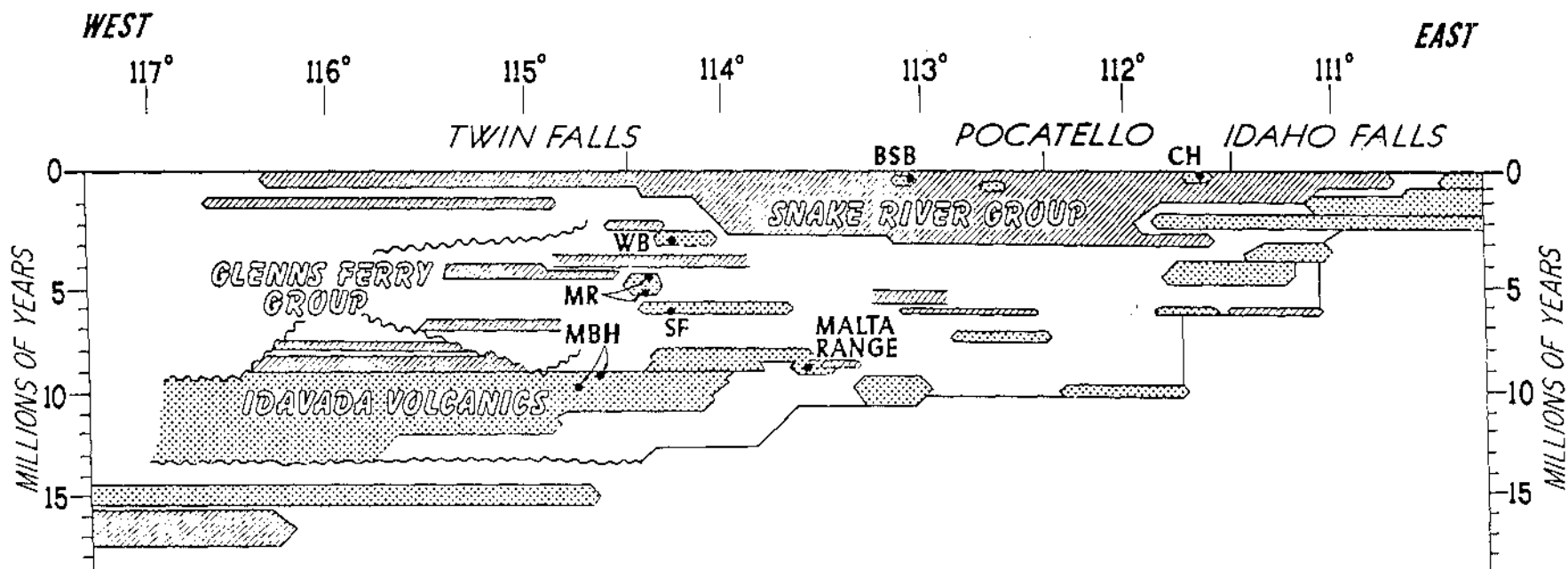


FIGURE 5.
SPACE-TIME PROFILE
OF VOLCANIC ROCKS
ALONG THE SNAKE RIVER
PLAIN, IDAHO (modified
after ARMSTRONG and others, 1980)



EXPLANATION

RHYOLITE
 BASALT

- BSB-BIG SOUTHERN BUTTE
- CH-CHINA HAT
- MBH-MOUNT BENNETT HILLS
- MR-MAGIC RESERVOIR
- SF-SHOSHONE FALLS
- WB-WEDGE BUTTE

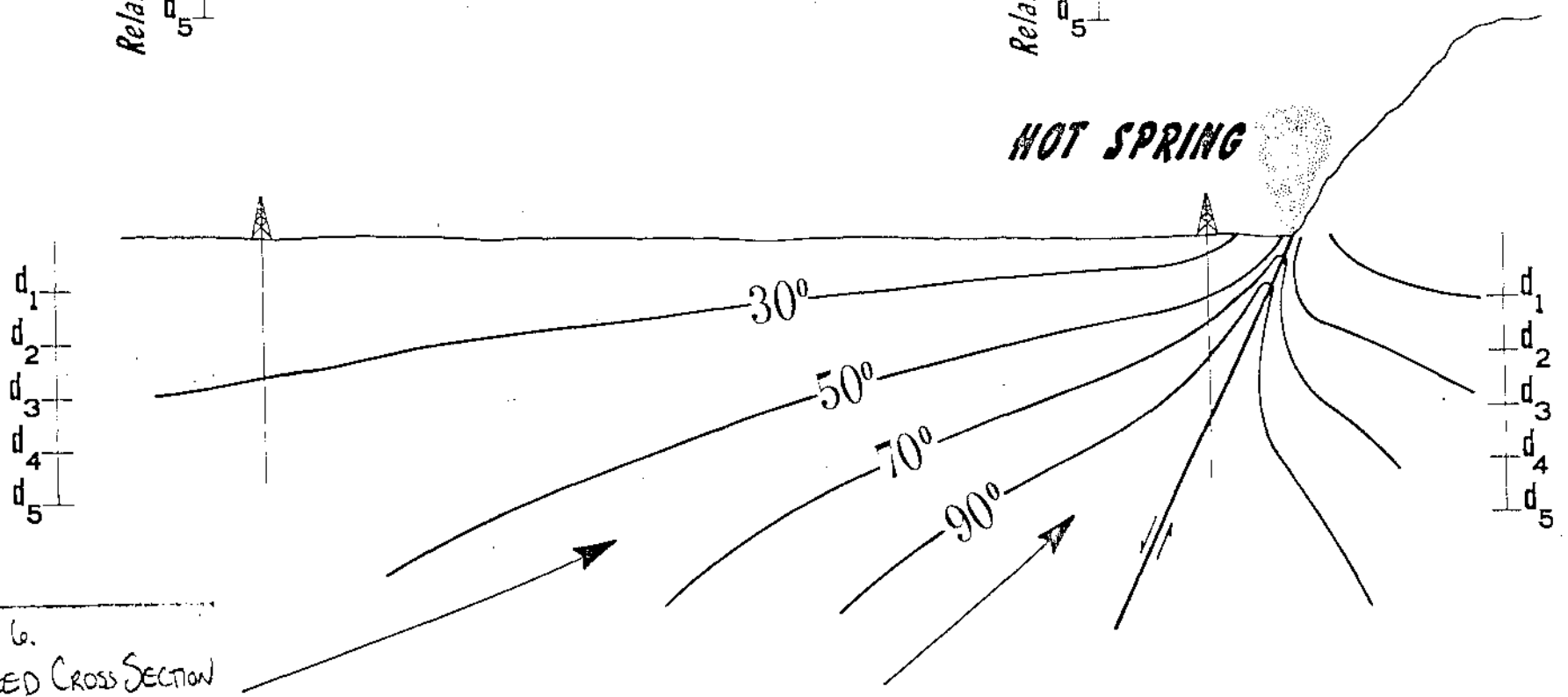
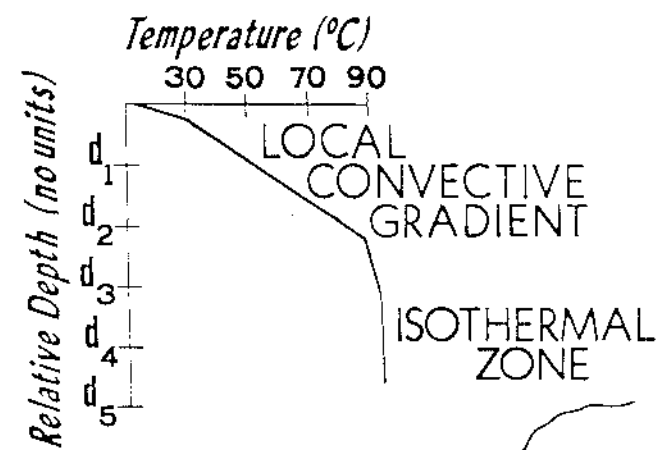
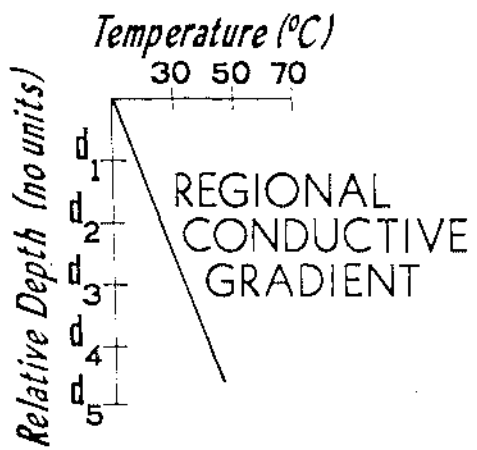


FIGURE 6.
IDEALIZED CROSS SECTION
AND TEMPERATURE-DEPTH
PROFILES OF A GEOTHERMAL
CONVECTION SYSTEM (isotherms
modified after Wilson and

FIGURE 7.
 THE RELATIONSHIP OF
 THEORETICAL CONDUCTIVE
 COOLING MODELS TO AGE,
 SIZE AND SHAPE OF
 SELECTED YOUNG IGNEOUS
 SYSTEMS IN IDAHO AND
 WYOMING (MODIFIED
 AFTER SMITH AND SHAW,
 1979)

